Supplementary Materials for

High-order fractal quantum oscillations in graphene/BN superlattices in the extreme doping limit

Wu Shi[1,2,3,4,5*], Salman Kahn[3,4,5], Nicolas Leconte[6], Takashi Taniguchi[7], Kenji Watanabe[7], Michael Crommie[3,4,5], Jeil Jung[6,8], Alex Zettl[3,4,5*]

[1]State Key Laboratory of Surface Physics and Institute for Nanoelectronic Devices and Quantum Computing, Fudan University, Shanghai 200433, China.

[2]Zhangjiang Fudan International Innovation Center, Fudan University, Shanghai 201210, China.

[3]Department of Physics, University of California, Berkeley, California 94720, USA.

[4]Materials Sciences Division, Lawrence Berkeley National Laboratory, Berkeley, California 94720, USA.

[5]Kavli Energy NanoSciences Institute at the University of California and the Lawrence Berkeley National Laboratory, Berkeley, California 94720, USA.

[6]Departmement of Physics, University of Seoul, Seoul 02504, Korea.

[7]National Institute for Materials Science, 1-1 Namiki, Tsukuba 305-0044, Japan.

[8]Department of Smart Cities, University of Seoul, Seoul 02504, Korea.

*Correspondence to: shiwu@fudan.edu.cn, azettl@berkeley.edu.

This PDF file includes:

Methods

Supplementary Figures

Methods

Device fabrication

High-quality h-BN crystals were supplied by Taniguchi and Watanabe. The h-BN/graphene/h-BN superlattices on 285nm SiO_2/Si substrates were fabricated using standard mechanical exfoliation and dry-transfer techniques [S1]. The thickness of h-BN flakes ranges from 8 to 40 nm. The top h-BN is mandatory as it protects the critical graphene layer from environmental surface contamination. During the dry-transfer process, we intentionally aligned the graphene's crystallographic axes with the bottom h-BN layer but misaligned it with the top h-BN layer. Standard electron-beam lithography processes were used to pattern the superlattices into Hall-bar devices with edge contacts (Fig. S1).

Electron-beam doping process

We use the recently developed electron-beam doping technique to achieve both high n- and p-type doping in graphene/h-BN heterostructures [S2]. All heterostructure devices were mounted in a SEM (model: FEI XL30 Sirion) using a custom holder attached to an electrical feedthrough for doping and in-situ electrical measurements. Electron-beam energies of 1keV to 30keV with beam current (I_e ~ 10 pA) and the normal scanning mode were used for electron-beam exposure. The typical exposure time t was ~ 60 s. The accumulated irradiation dosage D is given by $D = I_e t/Se$, where S is the exposure area. For $S = 300\ \mu m^2$, $D = 200\ \mu C cm^{-2} = 12.5\ e^- nm^{-2}$. We used a standard a.c. voltage bias lock-in technique to perform in-situ transport measurements of the devices in the SEM chamber under a vacuum of 3×10^{-6} mbar at room temperature.

Magneto-transport measurements

Low-temperature measurements were performed in a Quantum Design PPMS system after quickly transferring the doped sample from the SEM without significant exposure to ambient light. Such precautions were followed for all measurements reported in this work as light exposure to the doped sample might cause an additional photoinduced doping. Four-terminal resistances were measured using lock-in amplifiers (SRS 830) while the gate voltage was sourced through a Keithley source-meter (Keithley 2400).

Theoretical simulations

This wave packet method used here allows us to straightforwardly probe qualitatively different transport behaviors in the ballistic regime by following the mean quadratic displacement of the wave packets [S3–S5]. Note that the ballistic regime is often mostly avoided because the extracted conductivity will depend on the specific timestep of the evolution method making it difficult to make quantitative predictions. However, in this work we focus on this unusual regime allowing us to avoid the effects of disorder yet leveraging the fact that even in the ballistic regime, the conductivity captures the BZ oscillations qualitatively. We are not aware of other studies extracting the BZ oscillations in this way.

As this method gives access to the intensive conductivity observable, as opposed to Landauer formalism implementations which depend on the length of the system, in the ballistic regime we are limited to qualitative values of conductivity rather than a quantitatively well-defined number, by arbitrarily stopping the evolution of the wave packets after a large number of evolution steps. Such an approach proves itself able to clearly resolve BZ oscillations. The simulations occur at zero temperature, and thus can still resolve the Landau level features in the background. We use a reduced number of 2000 recursion steps to limit computation time needed to evaluate the mean-quadratic displacement at several time-steps on a 20-million atoms system to avoid spurious self-interacting wave-packet effects due to the periodic boundaries. The TB model itself is obtained by mapping out at the Brillouin-zone corner of graphene $K = (4\pi/3a\ \ G, 0)$ (with $a\ \ G$ the graphene lattice vector) [S3] a well-established continuum model given by $H = H\ \ 0(\vec{r})\sigma\ \ 0\tau\ \ 0 + H\ \ z(\vec{r})\sigma\ \ 3\tau\ \ 3 + \vec{H}_{xy}(\vec{r})\cdot\vec{\sigma}\tau\ \ 3$ with the pseudospin moire components $H_0(\vec{r}) = 2C_0 Re[f(\vec{r})e^{i\phi_0}]$and $H_z(\vec{r}) = 2C_z Re[f(\vec{r})e^{i\phi_z}]$for the diagonal terms and $H_{xy}(\vec{r}) = 2C_{xy}[cos\,(\phi)(\vec{z}\times 1) - sin\,(\phi)] \times \nabla Re[e^{i\phi_{xy}} f(\vec{r})]/|\vec{G}_1|$ for the off-diagonal terms [S6]. Diagonal terms are directly modifying the onsite energies of the TB model while for the off-diagonal terms, noting that $\vec{H}_{AB} = \vec{H}_{AB}{}^{\star}$, we can obtain the hBN-induced corrections δ_i to the graphene TB hopping terms using $\vec{H}_{AB} = \delta_1 - \frac{\delta_2+\delta_3}{2} + i\frac{\sqrt{3}}{2}(\delta_3 - \delta_2)$ leading to $\delta_1 = \frac{2}{3}Re(\vec{H}_{AB})$ and $\delta_{2,3} = \frac{-Re(\vec{H}_{AB})\pm\sqrt{3}Im(\vec{H}_{AB})}{3}$[3]. We use the rigid G/BN system parameters $C_0 = 10.13$ meV, $C_z = 9.01$ meV, $C_{xy} = 11.34$ meV, $\phi_0 = 146.53°$, $\phi_z = 68.43°$ and $\phi_{xy} = -109.6°$ [6].

Supplementary Figures

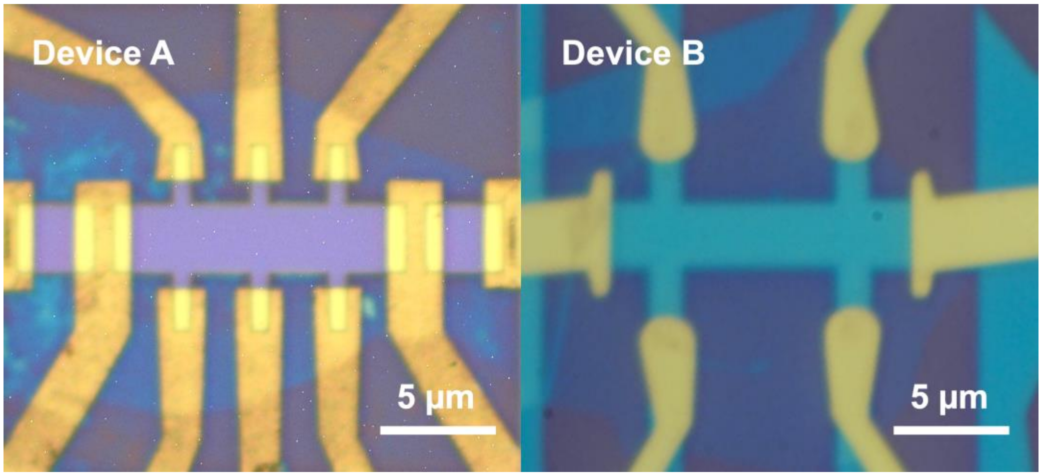

FIG. S1. Optical images of h-BN/graphene/h-BN superlattice devices. The superlattices (Device A and Device B) are shaped into Hall-bar geometry using standard electron beam lithography and reactive ion etching processes.

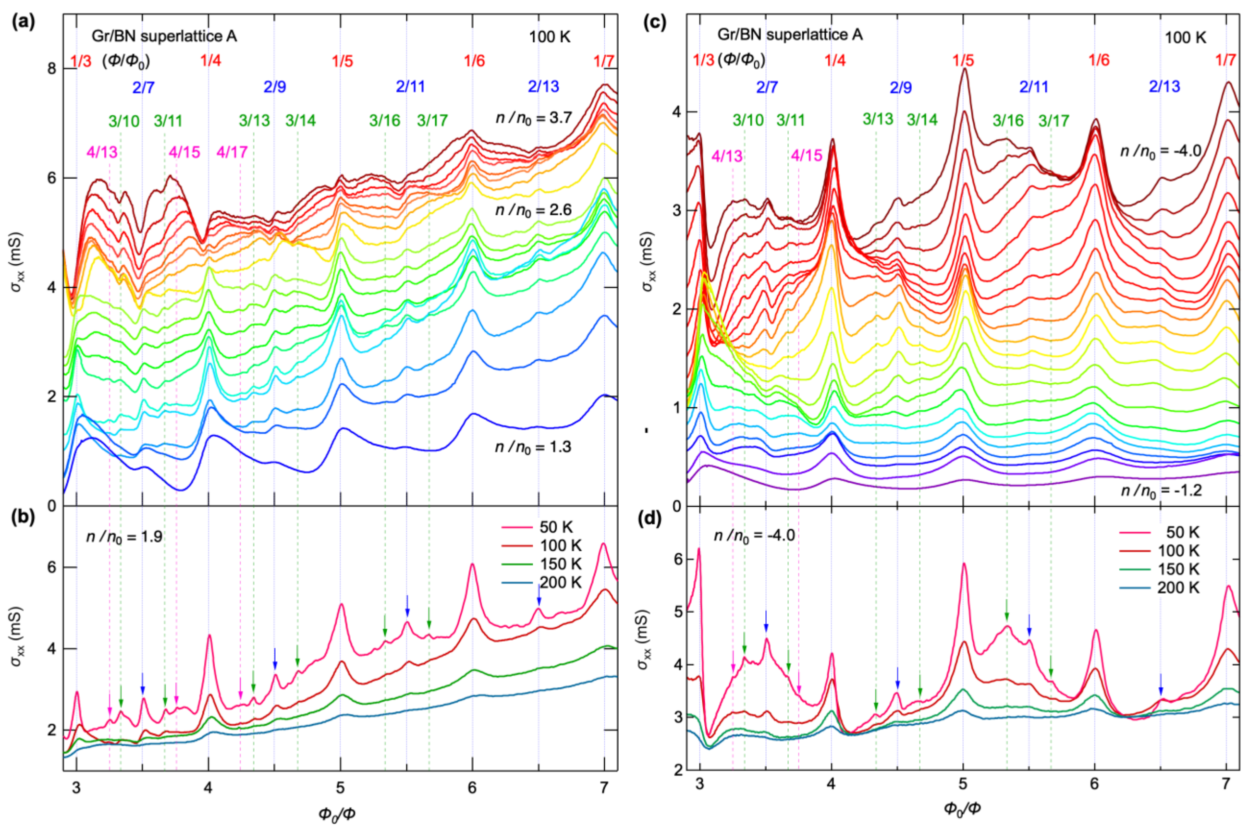

FIG. S2. High-order fractal BZ oscillations in highly electron-doped and hole-doped graphene/h-BN superlattice (Device A). (a) Longitudinal conductivity σ_{xx} as a function of ϕ_0/ϕ measured at various electron density n from $1.3n_0$ to $3.7n_0$ with a step of ~ $0.14n_0$. Here, the characteristic carrier density for the superlattice $n_0 = 2.3 \times 10^{12}$ cm^{-2}. (b) σ_{xx} as a function of ϕ_0/ϕ for electron density $n = 1.9n_0$ at various temperatures from 200 K to 50 K. (c) σ_{xx} as a function of ϕ_0/ϕ measured at various hole density n from $-1.2n_0$ to $-4.0n_0$ with a step of ~$0.14n_0$. (d) σ_{xx} as a function of ϕ_0/ϕ for hole density $n = -4.0\ n_0$ at various temperatures from 200 K to 50 K. The vertical dashed lines and arrows indicate the magnetic field positions where the fractal BZ states with p = 2, 3 and 4.

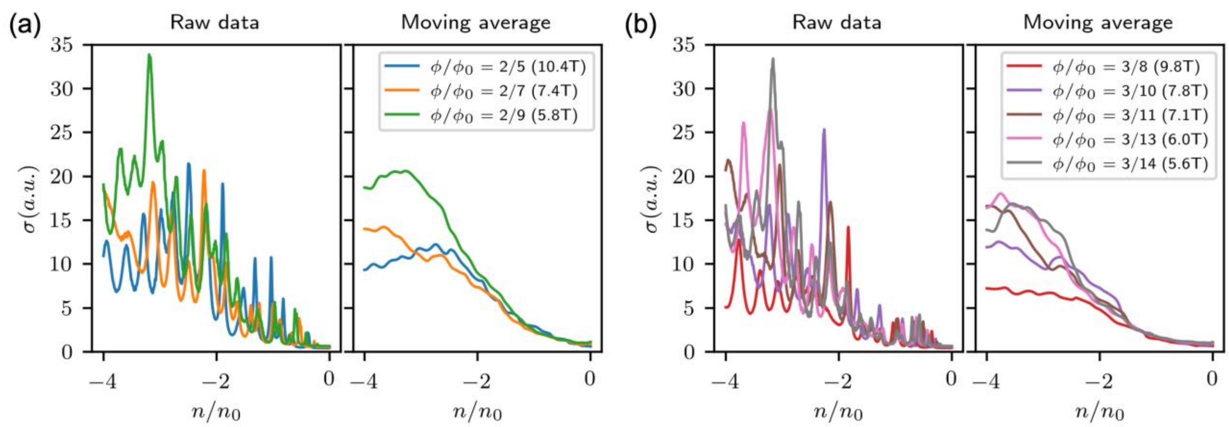

FIG. S3. Simulated magnetoconductivity as a function of carrier density at magnetic fields corresponding to selected fractal BZ states for hole-doped graphene/h-BN superlattices. Left panels in (a) and (b) are raw conductivity data extracted from Fig. 4(a) with (a) p = 2 and (b) p = 3. Right panels in (a) and (b) are obtained by taking a moving average of the data in left panels covering about 30 percent of the charge carrier density shown here. This allows dampening the Landau level oscillations while resolving the maximum in conductivity. The conductivity amplitude first increases with carrier density and then gradually decreases or saturates at around -3n_0, agreeing with experimental observations in Fig. 3(e).

References

[S1] L. Wang, I. Meric, P. Y. Huang, Q. Gao, Y. Gao, H. Tran, T. Taniguchi, K. Watanabe, L. M. Campos, D. A. Muller, J. Guo, P. Kim, J. Hone, K. L. Shepard, and C. R. Dean, Science **342**, 614 (2013).

[S2] W. Shi, S. Kahn, L. Jiang, S. Y. Wang, H. Z. Tsai, D. Wong, T. Taniguchi, K. Watanabe, F. Wang, M. F. Crommie, and A. Zettl, Nat. Electron. **3**, 99 (2020).

[S3] N. Leconte, A. Ferreira, and J. Jung, *Efficient Multiscale Lattice Simulations of Strained and Disordered Graphene*, 1st ed. (Elsevier Inc., 2016).

[S4] Z. Fan, J. H. Garcia, A. W. Cummings, J. E. Barrios-Vargas, M. Panhans, A. Harju, F. Ortmann, and S. Roche, Phys. Rep. **903**, 1 (2021).

[S5] N. Leconte, A. Lherbier, F. Varchon, P. Ordejon, S. Roche, and J. C. Charlier, Phys. Rev. B **84**, 235420 (2011).

[S6] J. Jung, E. Laksono, A. M. Dasilva, A. H. Macdonald, M. Mucha-Kruczyński, and S. Adam, Phys. Rev. B **96**, 085442 (2017).